

# Quadratic Characterizations for Reachability Analysis of Neural Networks

Elias Khalife, Mazen Farhood, and Pierre-Loic Garoche

**Abstract**—Quadratic constraints (QCs) are widely used to characterize nonlinearities and uncertainties, but generic analytical characterizations can be conservative on bounded domains. This paper develops a framework for constructing verified quadratic characterizations of scalar relations in the two-dimensional real plane. Candidate quadratic inequalities are locally generated by solving convex quadratic programs using samples from the relation and exterior sample points. They are then verified globally using sum-of-squares certificates over an exact semialgebraic description or, in the case of nonpolynomial relations, over relaxed polynomial descriptions. The resulting verified constraints define a sound overapproximation of the scalar relations over the considered domains. These constraints are directly compatible with existing analysis frameworks based on QCs and pointwise integral quadratic constraints (IQCs) for static nonlinearities and uncertainties, and they can also be embedded in QC-based semidefinite programs for reachability and safety analysis of feedforward neural networks. For smooth activations such as  $\tanh$ , the method yields domain-dependent quadratic characterizations that constitute an alternative to generic sector- or slope-based descriptions. For ReLU networks, we give methods to reduce conservatism in QC-based reachability analysis of feedforward networks by exploiting dependencies between neurons and tighter local bounds. Numerical examples demonstrate improved reachability results for smooth activations, reduced conservatism for ReLU networks, and applicability beyond neural networks through an example involving saturation.

## I. INTRODUCTION

In systems and control, quadratic constraints (QCs) are commonly used to characterize static input-output relations, including sector-bounded, slope-restricted, monotone, and repeated nonlinearities, as well as other static uncertainties [1]–[3]. QCs are also used in neural network verification and reachability analysis problems to characterize activation functions [4], [5]. Standard QC descriptions used in analysis are often derived analytically from broad structural properties of the underlying nonlinearity, such as sector, slope, monotonicity, or repetition conditions [2], [6]. These descriptions are convenient and often effective, but they are not, in general, tailored to a given static relation over a compact domain, which can lead to conservative analysis results. In this work, we seek a finite family of verified pointwise quadratic inequalities that defines a sound overapproximation of the relevant portion of the graph for a given static relation over a compact domain. This is motivated by applications in which only a bounded subset of the set of input-output pairs defining

the relation is relevant to the subsequent analysis. For example, a sector overapproximation of saturation may be overly conservative when restricted to a specific domain of interest. A similar issue arises in neural network reachability analysis, where admissible preactivation ranges are determined by the input set and the network parameters, so only bounded portions of the activation graphs need to be characterized.

This paper gives an approach for generating such QCs, which entails first generating candidate quadratic inequalities based on judiciously chosen sample points by solving convex quadratic programs, followed by verifying these inequalities using sum-of-squares certificates over an exact semialgebraic description of the relation or, in the nonpolynomial case, over a relaxed polynomial description [7], [8]. The resulting family of verified quadratic inequalities defines a sound outer approximation of the relation over the domain of interest and can be integrated into established QC-based and some IQC-based analysis methods [3], [9]. In this paper, we work out this integration for QC-based semidefinite programs arising in reachability and safety analysis problems of feedforward neural networks [4], [5]. For smooth activations such as  $\tanh$ , the proposed approach is used to generate the associated QCs, which can replace or complement generic analytical characterizations on the relevant bounded domains. For ReLU networks, the scalar ReLU graph already admits an exact quadratic characterization [4]. To reduce the conservatism in this case, we focus on combining this exact characterization with blockwise coupling of repeated ReLU units [10] and tightening of the neurons' pre- and post-activation bounds. Several examples are provided to demonstrate the generality and utility of the proposed approach in neural network and uncertain system analysis.

The remainder of the paper is organized as follows. Section II presents the notation and problem setup. Section III develops the sample-based candidate-generation and SOS-verification procedure. Section IV incorporates the verified quadratic characterizations into QC-based formulations for neural network reachability and safety analysis. Section V presents the ReLU-specific improvements. Section VI demonstrates the developed methods through examples, and Section VII concludes the paper.

## II. PRELIMINARIES

### A. Notation

The sets of real numbers, strictly positive integers,  $n$ -dimensional real vectors,  $n \times m$  real matrices, and  $n \times n$  real symmetric matrices are denoted by  $\mathbb{R}$ ,  $\mathbb{Z}_+$ ,  $\mathbb{R}^n$ ,  $\mathbb{R}^{n \times m}$ , and  $\mathbb{S}^n$ , respectively. The symbol  $I_n$  denotes the  $n \times n$  identity matrix, and  $\mathbf{1}$  denotes the vector of all ones. Subscripts indicating

E. Khalife and M. Farhood are with the Kevin T. Crofton Department of Aerospace and Ocean Engineering, Virginia Tech, Blacksburg, VA 24061, USA (e-mail: {eliask, farhood}@vt.edu). P.-L. Garoche is with the Federation ENAC ISAE-SUPAERO ONERA, Universite de Toulouse, Toulouse, France (e-mail: pierre-loic.garoche@enac.fr).

dimensions are omitted when clear from the context. For a matrix or vector  $X$ ,  $X^\top$  denotes its transpose. For a finite index set  $\mathcal{I}$ ,  $|\mathcal{I}|$  denotes its cardinality. For a symmetric matrix  $X \in \mathbb{S}^n$ , we write  $X > 0$  and  $X \geq 0$  to mean that  $X$  is positive definite and positive semidefinite, respectively, while  $X < 0$  and  $X \leq 0$  mean that  $X$  is negative definite and negative semidefinite, respectively.

The Euclidean norm of a vector  $x \in \mathbb{R}^n$  is denoted by  $\|x\|_2$ , i.e.,  $\|x\|_2 = (x^\top x)^{1/2}$ . For a polynomial variable  $z$ ,  $\mathbb{R}[z]$  denotes the ring of real polynomials in  $z$ , and  $\Sigma[z]$  denotes the cone of sum-of-squares polynomials in  $z$ .

### B. Problem Setup

Let  $\mathcal{S} \subset \mathbb{R}^2$  denote the set of admissible input-output pairs  $z = (x, y)$  satisfying a prescribed relation, and let  $\mathcal{D} \subset \mathbb{R}$  be a compact input domain. We denote by  $\mathcal{S}_{\mathcal{D}} := \{(x, y) \in \mathcal{S} \mid x \in \mathcal{D}\}$  the restriction of  $\mathcal{S}$  to  $\mathcal{D}$ . The relation may be specified by algebraic equalities and inequalities, logical conditions, piecewise functions, or any finite combination thereof. Our objective is to obtain a finite family of quadratic functions that are nonnegative on  $\mathcal{S}_{\mathcal{D}}$ .

To this end, define the quadratic monomial basis

$$\phi(z) := \begin{bmatrix} x^2 & y^2 & xy & x & y & 1 \end{bmatrix}^\top.$$

For  $i = 1, \dots, N_q$ , we consider the quadratic functions

$$q_i(z) = \begin{bmatrix} z^\top & 1 \end{bmatrix} Q_i \begin{bmatrix} z \\ 1 \end{bmatrix} = c_i^\top \phi(z),$$

where  $Q_i \in \mathbb{S}^3$ ,  $c_i \in \mathbb{R}^6$ , and  $N_q \in \mathbb{Z}_+$ . The family  $\{q_i\}_{i=1}^{N_q}$  is a quadratic characterization of  $\mathcal{S}_{\mathcal{D}}$  if

$$q_i(z) \geq 0, \quad \forall z \in \mathcal{S}_{\mathcal{D}}, \quad i = 1, \dots, N_q. \quad (1)$$

The associated set

$$\widehat{\mathcal{S}}_{N_q} := \{(x, y) \in \mathcal{D} \times \mathbb{R} \mid q_i(x, y) \geq 0, i = 1, \dots, N_q\}$$

is a sound overapproximation of  $\mathcal{S}_{\mathcal{D}}$  since  $\mathcal{S}_{\mathcal{D}} \subseteq \widehat{\mathcal{S}}_{N_q}$ .

Increasing the number of constraints  $N_q$  can improve the tightness of the overapproximation at the expense of added computational complexity in ensuing analysis. Therefore, the problem is to compute a verified quadratic characterization that balances the tightness of the overapproximation with the computational cost of the analysis.

## III. DATA-DRIVEN CANDIDATE GENERATION AND SOS VERIFICATION

The proposed approach consists of two stages. In the first stage, candidate quadratic constraints are generated from sampled data. In the second stage, each candidate is verified by solving SOS feasibility problems.

### A. Local decomposition, sampling, and candidate generation

Rather than constructing candidate quadratic functions on the entire  $\mathcal{S}_{\mathcal{D}}$ , we generate them on local restrictions of the relation. Let  $\mathcal{U}_k \subseteq \mathcal{D}$  be subdomains satisfying  $\mathcal{D} = \bigcup_{k=1}^{N_d} \mathcal{U}_k$  for some  $N_d \in \mathbb{Z}_+$ , and define  $\mathcal{S}_k := \mathcal{S}_{\mathcal{U}_k} = \{(x, y) \in \mathcal{S} \mid x \in \mathcal{U}_k\}$ . The subdomains do not have to be disjoint and are chosen to isolate local geometric features, such as smooth

branches, corners, switching regions, or junctions induced by piecewise or logical descriptions.

For each subdomain  $\mathcal{U}_k$ , we use three classes of sample points:

$$\begin{aligned} z_{k,j}^{\text{loc}} &\in \mathcal{S}_k, & j = 1, \dots, n_k^{\text{loc}}, \\ z_j^{\text{g}} &\in \mathcal{S}_{\mathcal{D}}, & j = 1, \dots, n^{\text{g}}, \\ z_{k,j}^{\text{ext}} &\notin \mathcal{S}, & j = 1, \dots, m_k, \end{aligned}$$

for some strictly positive integers  $n_k^{\text{loc}}$ ,  $n^{\text{g}}$ , and  $m_k$ , where  $k \in \{1, \dots, N_d\}$ . Here,  $z_{k,j}^{\text{loc}}$  are used to shape the candidate function on the local restriction  $\mathcal{S}_k$ , while  $z_j^{\text{g}}$  help enforce the required nonnegativity condition on  $\mathcal{S}_{\mathcal{D}}$ . The exterior samples  $z_{k,j}^{\text{ext}}$  are points outside  $\mathcal{S}$  where a negativity condition is imposed, typically chosen depending on the desired geometry of the resulting quadratic constraint. In practice, local samples are often placed near boundaries, transitions, corners, or other geometrically informative regions.

For each restriction  $\mathcal{S}_k$ , we compute a candidate function

$$q_k^{\text{cand}}(z) = c_k^\top \phi(z), \quad c_k \in \mathbb{R}^6, \quad (2)$$

by solving a convex quadratic program:

$$\begin{aligned} \min_{c_k, \xi_k^{\text{loc}}, \xi_k^{\text{g}}, \eta_k} \quad & \frac{\rho}{2} \|c_k\|_2^2 + \lambda_{\text{loc}} \mathbf{1}^\top \xi_k^{\text{loc}} + \lambda_{\text{g}} \mathbf{1}^\top \xi_k^{\text{g}} + \lambda_{\text{ext}} \mathbf{1}^\top \eta_k \\ \text{s.t.} \quad & c_k^\top \phi(z_{k,j}^{\text{loc}}) \geq \bar{\gamma} - \xi_{k,j}^{\text{loc}}, \quad j = 1, \dots, n_k^{\text{loc}}, \\ & c_k^\top \phi(z_j^{\text{g}}) \geq \bar{\gamma} - \xi_{k,j}^{\text{g}}, \quad j = 1, \dots, n^{\text{g}}, \\ & c_k^\top \phi(z_{k,j}^{\text{ext}}) \leq -\bar{\gamma} + \eta_{k,j}, \quad j = 1, \dots, m_k. \\ & \xi_k^{\text{loc}} \geq 0, \quad \xi_k^{\text{g}} \geq 0, \quad \eta_k \geq 0, \end{aligned} \quad (3)$$

where  $\bar{\gamma} > 0$  is a prescribed margin,  $\lambda_{\text{loc}}, \lambda_{\text{g}}, \lambda_{\text{ext}} > 0$  are user-selected weights,  $\rho > 0$  is a regularization parameter that penalizes the magnitudes of the coefficient vectors, and  $\xi_k^{\text{loc}} \in \mathbb{R}^{n_k^{\text{loc}}}$ ,  $\xi_k^{\text{g}} \in \mathbb{R}^{n^{\text{g}}}$ , and  $\eta_k \in \mathbb{R}^{m_k}$  are nonnegative vectors included to allow potential violations at certain sample points. The size of problem (3) scales linearly with  $(n_k^{\text{loc}} + n^{\text{g}} + m_k)$ .

Multiple candidate quadratic functions may be computed for a local restriction  $\mathcal{S}_k$  depending on the local geometry of the relation and on whether the desired QCs are intended to lead to tighter lower or upper bounds. For instance, one may compute separate candidate functions to specify the lower- and upper-bounding curves for the overapproximation of  $\mathcal{S}_k$ , with the sample sets selected accordingly. However, regardless of the sampling strategy, solving (3) only enforces the prescribed inequalities on finitely many samples and does not guarantee that  $q_k^{\text{cand}}(z) \geq 0$  for all  $z \in \mathcal{S}_{\mathcal{D}}$ . A separate verification step is required to ensure global validity on  $\mathcal{S}_{\mathcal{D}}$ .

### B. SOS-based verification

1) *Piecewise-polynomial relations:* Suppose that the set  $\mathcal{S}_{\mathcal{D}}$  is defined by a piecewise-polynomial relation, i.e.,  $\mathcal{S}_{\mathcal{D}} = \{(x, y) \in \mathcal{D} \times \mathbb{R} \mid P(x, y) = 0\}$ , where  $P(\cdot, \cdot)$  is a piecewise polynomial function. In this case,  $\mathcal{S}_{\mathcal{D}}$  can be represented exactly by a semialgebraic set or a union of semialgebraic sets. Assume  $\mathcal{S}_{\mathcal{D}}$  is expressed as a union of  $N_s$  semialgebraic sets for some  $N_s \in \mathbb{Z}_+$ , i.e.,

$$\mathcal{S}_{\mathcal{D}} = \bigcup_{i=1}^{N_s} \mathcal{S}^{(i)},$$

where  $\mathcal{S}^{(i)} = \{z \in \mathbb{R}^2 \mid g_j^{(i)}(z) \geq 0, j = 1, \dots, m_i\}$  and  $i = 1, \dots, N_s$ . A candidate quadratic  $q_k^{\text{cand}}$  is verified by solving the SOS feasibility problem on each subset  $\mathcal{S}^{(i)}$ . Specifically, for each  $i = 1, \dots, N_s$ , we solve the SOS feasibility problem

$$\begin{aligned} & \text{find } \sigma_{1,k}^{(i)}, \dots, \sigma_{m_i,k}^{(i)} \\ & \text{s.t. } \sigma_{j,k}^{(i)} \in \Sigma[z], \quad j = 1, \dots, m_i, \\ & q_k^{\text{cand}}(z) - \sum_{j=1}^{m_i} \sigma_{j,k}^{(i)}(z) g_j^{(i)}(z) \in \Sigma[z]. \end{aligned} \quad (4)$$

If (4) is feasible for every  $i \in \{1, \dots, N_s\}$ , then  $q_k^{\text{cand}}(z) \geq 0$  for all  $z \in \mathcal{S}_{\mathcal{D}}$ .

Let  $\mathcal{Q}_{\text{cert}}$  denote the set of the  $N_q$  candidate quadratic functions that pass the SOS verification step. Then,  $\mathcal{Q}_{\text{cert}}$  defines a verified quadratic characterization of  $\mathcal{S}_{\mathcal{D}}$ , and the set  $\tilde{\mathcal{S}}_{N_q} := \{(x, y) \in \mathcal{D} \times \mathbb{R} \mid q(x, y) \geq 0 \text{ for all } q \in \mathcal{Q}_{\text{cert}}\}$  is a sound overapproximation of  $\mathcal{S}_{\mathcal{D}}$ , i.e.,  $\mathcal{S}_{\mathcal{D}} \subseteq \tilde{\mathcal{S}}_{N_q}$ .

*Remark 1:* As an alternative to SOS verification, the soundness of the overapproximation can also be established by SMT-based verification [11], which can account for floating-point roundoff errors (see [12], [13]), and by a machine-checked proof in an interactive theorem prover such as Rocq [14].

*Remark 2:* The domain used for candidate generation and the domain used for verification do not need to be identical. In particular, candidates may be generated on  $\mathcal{D}$  and then verified on a larger domain  $\tilde{\mathcal{D}} \supseteq \mathcal{D}$ .

*Remark 3:* If  $\mathcal{S}$  has a known symmetry, candidate generation and verification can be restricted to a representative subset of the domain, and the remaining candidates can be obtained by symmetry. This reduces the number of candidate generation and SOS verification problems.

2) *Nonpolynomial relations:* When the relation defining  $\mathcal{S}_{\mathcal{D}}$  is not piecewise-polynomial, the verification step is handled differently. The candidate generation step remains data-driven and can involve samples from the exact relation. However, SOS verification requires representing the set  $\mathcal{S}_{\mathcal{D}}$  using polynomial constraints. Therefore, a polynomial approximation is introduced in the verification step, along with a bound on the approximation error.

Consider the set

$$\mathcal{S}_{\mathcal{D}} := \{(x, y) \in \mathbb{R}^2 \mid y = \varphi(x), x \in \mathcal{D}\},$$

where  $\varphi: \mathbb{R} \rightarrow \mathbb{R}$  is a nonpolynomial function. Let  $p$  be a polynomial approximation of  $\varphi$  on  $\mathcal{D}$ , and suppose that an error bound  $\varepsilon \geq 0$  is available such that

$$|\varphi(x) - p(x)| \leq \varepsilon \text{ for all } x \in \mathcal{D}.$$

We then define the relaxed verification set

$$\tilde{\mathcal{S}}_{p,\varepsilon,\mathcal{D}} := \{(x, y) \in \mathbb{R}^2 \mid x \in \mathcal{D}, -\varepsilon \leq y - p(x) \leq \varepsilon\}.$$

Since  $\mathcal{S}_{\mathcal{D}} \subseteq \tilde{\mathcal{S}}_{p,\varepsilon,\mathcal{D}}$ , the verification of a candidate quadratic function on  $\tilde{\mathcal{S}}_{p,\varepsilon,\mathcal{D}}$  carries over to  $\mathcal{S}_{\mathcal{D}}$ . The error bound may be derived analytically, for example, from Taylor remainder estimates, or obtained using uniform approximation methods such as Chebyshev minimax polynomial approximation [15].

The approximation is not necessarily constructed over the entire domain  $\mathcal{D}$  at once. If  $\mathcal{D} = \bigcup_{i=1}^{N_e} \mathcal{D}_i$  for some  $N_e \in \mathbb{Z}_+$ , one may instead use polynomial approximations  $p_i$  with error bounds  $\varepsilon_i$  on the subsets  $\mathcal{D}_i$  and verify the candidate on the corresponding relaxed verification sets  $\tilde{\mathcal{S}}_{p_i,\varepsilon_i,\mathcal{D}_i}$ . Verification on all such sets implies verification on  $\mathcal{S}_{\mathcal{D}}$ . This approach is used in the tanh example in Section VI.

#### IV. APPLICATION TO FEEDFORWARD NEURAL NETWORK REACHABILITY ANALYSIS

In this section, we show how the verified quadratic functions constructed in Section III can be incorporated into an existing QC-based semidefinite program (SDP) formulation for reachability analysis and safety verification of feedforward neural networks, such as the framework in [4].

##### A. Network model and safety verification

Consider a feedforward neural network with  $L$  hidden layers. Let  $x \in \mathbb{R}^{n_x}$  denote the input,  $\varphi^\ell, \vartheta^\ell \in \mathbb{R}^{n_\ell}$  denote the preactivation and postactivation vectors of layer  $\ell$ , and  $y \in \mathbb{R}^{n_y}$  denote the output. We write the network as

$$\begin{aligned} \vartheta^0 &= x, \\ \varphi^\ell &= W^\ell \vartheta^{\ell-1} + b^\ell, \quad \ell = 1, \dots, L, \\ \vartheta^\ell &= \sigma(\varphi^\ell), \quad \ell = 1, \dots, L, \\ y &= W^{L+1} \vartheta^L + b^{L+1}, \end{aligned}$$

where  $W^\ell \in \mathbb{R}^{n_\ell \times n_{\ell-1}}$ ,  $b^\ell \in \mathbb{R}^{n_\ell}$  for  $\ell = 1, \dots, L$ , and  $W^{L+1} \in \mathbb{R}^{n_y \times n_L}$ ,  $b^{L+1} \in \mathbb{R}^{n_y}$ . The scalar activation is denoted by  $\sigma: \mathbb{R} \rightarrow \mathbb{R}$ , and  $\sigma$  is the corresponding componentwise map,

$$\sigma(v) := [\sigma(v_1) \quad \dots \quad \sigma(v_n)]^\top, \quad v \in \mathbb{R}^n.$$

For clarity, the formulation is presented for a common activation function  $\sigma$  across the hidden layers. The extension to layer- or neuron-dependent activations is immediate.

Let  $\mathcal{X} := \{x \in \mathbb{R}^{n_x} \mid [x \ 1] P_i [x \ 1]^\top \geq 0 \text{ for } i = 1, \dots, N_x\}$ , for some  $N_x \in \mathbb{Z}_+$  and  $P_i \in \mathbb{S}^{n_x+1}$ , be a bounded admissible input set and  $\mathcal{Y}$  its associated output reachable set, i.e.,

$$\mathcal{Y} := \{y \in \mathbb{R}^{n_y} \mid y = f(x), x \in \mathcal{X}\},$$

where  $f$  denotes the input-output map of the network and is bounded on  $\mathcal{X}$ . Define the function  $b^*: \mathbb{R}^{n_y} \rightarrow \mathbb{R}$  by

$$b^*(a) := \sup_{x \in \mathcal{X}} a^\top f(x).$$

Then, clearly, for any upper bound  $\bar{b}_a \geq b^*(a)$ , the halfspace  $\mathcal{H}_{\bar{b}_a} := \{y \in \mathbb{R}^{n_y} \mid a^\top y \leq \bar{b}_a\}$  is a superset of  $\mathcal{Y}$ , i.e.,  $\mathcal{Y} \subseteq \mathcal{H}_{\bar{b}_a}$ . Thus, given prescribed directions  $a_i \in \mathbb{R}^{n_y}$ ,  $i = 1, \dots, N_{\text{dir}}$  for some  $N_{\text{dir}} \in \mathbb{Z}_+$ , a polytopic outer approximation is given by

$$\mathcal{Y} \subseteq \{y \in \mathbb{R}^{n_y} \mid a_i^\top y \leq \bar{b}_{a_i}, i = 1, \dots, N_{\text{dir}}\}.$$

There are available methods, such as the one in [4], that provide appropriate upper bounds  $\bar{b}_{a_i}$  (the minimal values afforded by the used method). If the network's safety requirement can be expressed in terms of a set of linear inequalities,  $a_{\text{safe},i}^\top y \leq b_{\text{safe},i}$ , then verifying safety entails showing that the safety region defined by these inequalities is a superset

of the aforementioned polytopic outer approximation, i.e.,  $\bar{b}_{a_{\text{safe},i}} \leq b_{\text{safe},i}$ , where  $\bar{b}_{a_{\text{safe},i}}$  is obtained by applying a reachability analysis result. Alternatively, the safety conditions can be incorporated directly into the reachability analysis problem, and then safety is proved by solving a feasibility problem. The same framework also supports other safety and outer approximation set descriptions, such as ellipsoids [4].

### B. QC-based SDP formulation

Let  $\mathbb{Q}_{\text{cert}} \subset \mathbb{S}^3$  denote the set of symmetric matrices associated with the verified quadratic functions in  $\mathbb{Q}_{\text{cert}}$ . The scalar activation  $\sigma$  is said to satisfy the QCs defined by  $\mathbb{Q}_{\text{cert}}$  if, for every pair  $(h_1, h_2)$  satisfying  $h_2 = \sigma(h_1)$ ,

$$\begin{bmatrix} h_1 & h_2 & 1 \end{bmatrix} Q \begin{bmatrix} h_1 \\ h_2 \\ 1 \end{bmatrix} \geq 0 \text{ for all } Q \in \mathbb{Q}_{\text{cert}}.$$

If that is the case, then  $\sigma$  also satisfies the QCs defined by the conic hull of  $\mathbb{Q}_{\text{cert}}$ .

Similarly to [4], we define the lifted vector

$$\xi := \begin{bmatrix} x^\top & (\vartheta^1)^\top & \dots & (\vartheta^L)^\top & 1 \end{bmatrix}^\top,$$

along with extraction matrices to recover the variables of interest from the lifted vector. Specifically, let  $E_x \xi = \begin{bmatrix} x & 1 \end{bmatrix}^\top$ ,  $E_y \xi = \begin{bmatrix} y & 1 \end{bmatrix}^\top$ , and  $E_i^\ell \xi = \begin{bmatrix} \varphi_i^\ell & \vartheta_i^\ell & 1 \end{bmatrix}^\top$  for each neuron  $i$  in layer  $\ell$ . These matrices are constructed based on the network weights, biases, and the definition of  $\xi$ .

The linear matrix inequality from the reachability analysis SDP in [4] follows from the S-procedure [16] and has the form

$$M_x + M_\sigma + M_y \leq 0, \quad (5)$$

where the dependence of the first two terms on multipliers is suppressed for simplicity. Here,  $M_x = E_x^\top \left( \sum_{i=1}^{N_x} \tau_i P_i \right) E_x$ , with  $\tau = [\tau_1 \dots \tau_{N_x}]^\top$  denoting the vector of nonnegative multipliers, corresponds to the input-set constraints,  $M_\sigma$  corresponds to the activation-related quadratic constraints, and  $M_y$  corresponds to the conditions defining the overapproximated output set or the output safety constraints. The admissible input set  $\mathcal{X}$ , the overapproximated output set, and the safety region are typically described by hyperrectangles, polytopes, or ellipsoids, all of which can be handled within this QC-based SDP framework [4]. In the polytopic case, the normal vectors to the polytope facets are prescribed by the user.

The verified quadratic characterizations derived in Section III are incorporated into the framework via the matrix

$$M_{\text{cert}}(\Lambda) = \sum_{\ell=1}^L \sum_{i=1}^{n_\ell} \sum_{r=1}^{N_{\ell,i}} \lambda_{\ell,i,r} (E_i^\ell)^\top Q_{\ell,i,r} E_i^\ell,$$

where  $\Lambda$  denotes the vector of the nonnegative multipliers  $\lambda_{\ell,i,r}$  associated with the verified scalar quadratic constraints, and  $\{Q_{\ell,i,r}\}_{r=1}^{N_{\ell,i}}$  denotes the family of symmetric matrices defining the verified scalar QCs assigned to neuron  $i$  in layer  $\ell$ . In the common case where all neurons share the same activation function and the same verified family of QCs, we have  $N_{\ell,i} = N_q$  and  $Q_{\ell,i,r} = Q_r$  for all  $\ell$  and  $i$  so that the verified QC family is identical across the network, while the multipliers remain neuron/layer-dependent.

Multiple activation characterizations or properties can be combined within the overall activation block  $M_\sigma$ . For example, local bounds on preactivations or postactivations can be encoded as quadratic inequalities and added to the formulation. Accordingly, we write

$$M_\sigma = M_{\text{cert}}(\Lambda) + M_{\text{loc}}(\nu) + \dots, \quad (6)$$

where  $M_{\text{loc}}(\nu)$ , with  $\nu$  denoting the vector of nonnegative multipliers, corresponds to the local-bound constraints, and the rest of the terms correspond to any other valid constraints.

The following proposition follows from the results of [4], [5]. It addresses the computation of a polytopic overapproximation for the output reachable set.

*Proposition 1 ([4], [5]):* Let  $a_j \in \mathbb{R}^{n_y}$  be a normal vector to facet  $j$  of the overapproximating polytope, and define

$$S(a_j, b_j) := \begin{bmatrix} 0 & a_j \\ a_j^\top & -2b_j \end{bmatrix}.$$

Then, the offset  $b_j$  that, together with the normal vector  $a_j$ , defines the hyperplane  $\{y \in \mathbb{R}^{n_y} \mid a_j^\top y = b_j\}$  containing the facet is obtained by solving the following optimization problem:

$$\begin{aligned} \min_{b_j, \Lambda, \nu, \tau, \dots} \quad & b_j \\ \text{s.t.} \quad & M_x + M_\sigma + E_y^\top S(a_j, b_j) E_y \leq 0, \\ & \Lambda \geq 0, \quad \nu \geq 0, \quad \tau \geq 0, \quad \dots, \end{aligned} \quad (7)$$

where the inequality  $\geq$  holds elementwise. Solving (7) over the selected family of facet normal vectors yields a polytopic overapproximation of the output reachable set.

Clearly, pre- and post-multiplying the matrix inequality in (7) by  $\xi^\top$  and  $\xi$ , respectively, and observing that both  $\xi^\top M_x \xi$  and  $\xi^\top M_\sigma \xi$  are nonnegative for every admissible trajectory, we can conclude that  $\xi^\top E_y^\top S(a_j, b_j) E_y \xi \leq 0$ , or equivalently,  $a_j^\top y \leq b_j$  holds for all  $x \in \mathcal{X}$ .

For safety verification, we first consider the case of a single linear inequality  $c^\top y \leq d$ . This property can be checked by solving the following SDP feasibility problem:

$$\begin{aligned} \text{find} \quad & \Lambda, \nu, \tau \dots \\ \text{s.t.} \quad & M_x + M_\sigma + E_y^\top S(c, d) E_y \leq 0, \\ & \Lambda \geq 0, \quad \nu \geq 0, \quad \tau \geq 0, \quad \dots \end{aligned} \quad (8)$$

If (8) is feasible, the inequality  $c^\top y \leq d$  holds for all  $x \in \mathcal{X}$ . More general polyhedral safety constraints can be handled by iteratively applying this procedure to each defining inequality.

*Remark 4:* The preceding construction is not restricted to feedforward neural networks. More generally, any analysis framework for uncertain or nonlinear systems that models a relation of the form  $\vartheta = \Delta(\varphi)$  through pointwise IQCs can, in principle, use the verified quadratic characterizations developed in Section III, provided the relation is represented on a suitable bounded operating domain. This includes, for example, QC-based procedures for reachability analysis, invariant-set computation, and safety verification.

The same idea also extends to formal-verification settings in which quadratic constraints are used as annotations or preconditions. In particular, [13] uses deductive verification

and SMT-based reasoning to verify systemic properties of control programs. The verified quadratic characterizations developed in this work can be incorporated in a similar manner within such QC-based annotation frameworks.

## V. RELU-SPECIFIC TIGHTENING FOR FEEDFORWARD NEURAL NETWORK REACHABILITY ANALYSIS

The previous section showed how verified quadratic characterizations can be embedded in a QC-based SDP for reachability analysis of feedforward neural networks. For ReLU networks, however, the method given in Section III is not needed since the scalar ReLU graph already admits an exact quadratic description. In this case, the main sources of conservatism are the treatment of neurons as independent units and the overapproximation of local bounds. This section introduces ReLU-specific improvements based on exact scalar constraints, blockwise repeated-ReLU coupling, local bound tightening, and neuron pruning.

### A. ReLU characterizations

The graph of the scalar ReLU relation,  $\vartheta = \text{ReLU}(\varphi) = \max(0, \varphi)$ , is characterized exactly by

$$\vartheta \geq 0, \quad \vartheta \geq \varphi, \quad \vartheta(\varphi - \vartheta) \geq 0. \quad (9)$$

When imposed separately on each preactivation-postactivation pair, this exact scalar characterization treats the ReLU units independently and does not capture relations among neuron activations, which introduces conservatism in the SDP relaxation. Repeated-nonlinearity QCs, as in [4], partially address this issue by correlating repeated copies of the same activation, thereby reducing conservatism at an increased computational cost. A more recent result in [10] derives a complete QC characterization for repeated ReLU in terms of matrix copositivity conditions. However, directly applying this complete characterization across all hidden-layer units remains computationally prohibitive.

To maintain tractability, we employ a relaxed blockwise construction. Let  $\varphi_r, \vartheta_r \in \mathbb{R}^{n_r}$  consist of the preactivation and postactivation variables of the ReLU units included in the repeated characterization. Let  $\mathcal{I}_1, \dots, \mathcal{I}_{N_b}$  be partitions of  $\{1, \dots, n_r\}$  for some  $N_b \in \mathbb{Z}_+$ , with

$$|\mathcal{I}_i| \leq s_{\max}, \quad i = 1, \dots, N_b,$$

where  $s_{\max}$  is a user-specified maximum block size. From [10], for each block  $\mathcal{I}_i$ , we impose a repeated-ReLU QC defined by a matrix of the form

$$M_{\text{rep}}^{(i)} = M_1^{(i)} + (T^{(i)})^\top Q_2^{(i)} T^{(i)}, \quad (10)$$

where

$$M_1^{(i)} := \begin{bmatrix} 0 & Q_1^{(i)} \\ Q_1^{(i)} & -2Q_1^{(i)} \end{bmatrix}, \quad T^{(i)} := \begin{bmatrix} -I_{|\mathcal{I}_i|} & I_{|\mathcal{I}_i|} \\ 0 & I_{|\mathcal{I}_i|} \end{bmatrix},$$

and  $Q_1^{(i)}$  is a diagonal matrix variable. The copositive constraint on the matrix variable  $Q_2^{(i)}$  is relaxed by introducing the variable  $N_2^{(i)}$  and imposing

$$Q_2^{(i)} - N_2^{(i)} \geq 0, \quad N_2^{(i)} = (N_2^{(i)})^\top \geq 0, \quad (11)$$

where  $N_2^{(i)} \geq 0$  holds elementwise. After pre- and post-multiplying (10) by the appropriate extraction matrices, the resulting terms are added to the expression for  $M_\sigma$  in (6). The blockwise repeated-ReLU characterization retains relations between neuron activations while keeping the SDP tractable. The blocks can be formed sequentially on the stacked index set and are therefore not restricted to a single layer.

*Remark 5:* An alternative to sequential block formation is to group neurons within each layer according to the cosine similarity of their incoming weight vectors. For neurons  $i$  and  $j$  in layer  $\ell$ , with  $W_i^\ell$  and  $W_j^\ell$  denoting the  $i$ th and  $j$ th rows of  $W^\ell$ , we can evaluate  $\text{sim}_{ij}^\ell := \frac{(W_i^\ell)(W_j^\ell)^\top}{\|W_i^\ell\|_2 \|W_j^\ell\|_2}$  and prioritize block grouping for highly similar neurons.

### B. Local bounds and pruning

A second source of conservatism is the overapproximation of local neuron bounds. Let  $\underline{\varphi}_i^\ell \leq \varphi_i^\ell \leq \overline{\varphi}_i^\ell$  denote local preactivation bounds for neuron  $i$  in layer  $\ell$ . Such bounds may be computed inexpensively by interval bound propagation (IBP) and incorporated into the SDP through quadratic box constraints, for example,

$$(\varphi_i^\ell - \underline{\varphi}_i^\ell)(\overline{\varphi}_i^\ell - \varphi_i^\ell) \geq 0, \quad (\vartheta_i^\ell - \underline{\vartheta}_i^\ell)(\overline{\vartheta}_i^\ell - \vartheta_i^\ell) \geq 0.$$

These local bounds also enable pruning. If  $\overline{\varphi}_i^\ell \leq 0$ , then neuron  $i$  is always inactive and  $\vartheta_i^\ell = 0$ . Such a neuron can be removed from the analysis, and its contribution can be eliminated by removing the corresponding row from the current-layer representation and the corresponding column from the next-layer weight matrix. If  $\underline{\varphi}_i^\ell \geq 0$ , then neuron  $i$  is always active and  $\vartheta_i^\ell = \varphi_i^\ell$ , i.e., the ReLU nonlinearity can be replaced with the identity relation. Only unstable neurons, i.e., neurons satisfying  $\underline{\varphi}_i^\ell < 0 < \overline{\varphi}_i^\ell$ , need to be characterized. This pruning step improves both computational efficiency and analysis outcomes. It reduces the SDP dimension by eliminating neurons whose activation mode is already determined and avoids the conservatism resulting from applying the ReLU characterization to neurons whose exact behavior is known.

### C. Local bound tightening

Although IBP is inexpensive, it suffers from the wrapping effect; as the depth increases, the propagated interval boxes become conservative because relations among neuron activations are ignored. In particular, IBP may admit combinations of neuron values that are individually feasible but not jointly realizable by the network. To mitigate this effect, we use a procedure for propagating bounding polytopes across the hidden layers. At each hidden layer  $\ell$ , we compute a postactivation polytope  $\mathcal{P}^\ell := \{\vartheta^\ell \in \mathbb{R}^{n_\ell} \mid A^\ell \vartheta^\ell \leq b^\ell\}$ , where the inequality is applied elementwise, the matrix  $A^\ell$  is prescribed, and the vector  $b^\ell$  contains the tightest valid bounds, computed one bound at a time using the same QC-based SDP framework. The normal vectors to the polytope facets, i.e., the rows of  $A^\ell$ , may be selected progressively. At least two normal vectors are chosen for each neuron  $i$ , namely,  $e_i$  and  $-e_i$ , where  $e_i$  is the  $i^{\text{th}}$  standard basis vector. This minimal choice yields componentwise bounds. Tighter descriptions are obtained by adding normal vectors such as

- 1) the right-singular vectors corresponding to the  $t$  largest singular values, for some  $t$ , of the next-layer weight matrix obtained from singular value decomposition, which help capture directions most relevant for propagation through the subsequent linear map [17];
- 2) the vectors  $\pm e_i \pm e_j$ , which encode pairwise relations between neurons.

Additional facet families may be included in the same manner. In general, a richer facet set yields a tighter propagated polytope at a higher computational cost.

Once  $\mathcal{P}^\ell$  is available, it is used to tighten the next-layer preactivation bounds by solving linear programs. For each neuron  $i$  in layer  $\ell + 1$ , we solve for

$$\begin{aligned}\underline{\varphi}_{i,\text{LP}}^{\ell+1} &= \min_{\vartheta^\ell \in \mathcal{P}^\ell} (W_i^{\ell+1} \vartheta^\ell + b_i^{\ell+1}), \\ \overline{\varphi}_{i,\text{LP}}^{\ell+1} &= \max_{\vartheta^\ell \in \mathcal{P}^\ell} (W_i^{\ell+1} \vartheta^\ell + b_i^{\ell+1}).\end{aligned}$$

The intersections of the obtained preactivation/postactivation intervals and the current intervals obtained from IBP generally yield improved bounds, which strengthen the local box constraints, enable additional pruning, and improve the polytope computed at the next layer. The procedure is repeated sequentially through the network.

In the polytope-propagation problems at the hidden layers, we use the exact scalar characterization together with the local bound constraints. At this stage, each additional normal vector already requires a separate SDP, and the added cost of block-repeated coupling is typically not justified by the resulting improvement in the propagated hidden-layer bounds. In the final output-reachability computation, however, the combined characterization is preferred: the exact scalar constraints enforce the exact graph of each ReLU unit, the block-repeated constraints capture relations among subsets of unstable neurons, and the propagated local bounds further restrict the feasible set. Among the tractable formulations considered, this yields the tightest output bounds.

*Remark 6:* In branch-and-bound implementations, the expensive SDP-based layerwise polytope propagation can be executed solely as root-level preprocessing; because child subdomains are subsets of the root domain, these initial bounds remain trivially valid for all descendant nodes.

## VI. EXAMPLES

In this section, we apply the proposed methods to scalar nonlinearities, an uncertain-system example with saturation, and neural-network reachability and verification problems.

### A. Quadratic characterizations of scalar nonlinearities

We apply the proposed data-driven candidate-generation and verification procedure to two scalar relations. The resulting quadratic characterizations are shown in Fig. 1.

- 1) *Hyperbolic tangent:* Consider the set

$$\mathcal{S}_{\tanh} := \{(\varphi, \vartheta) \in \mathbb{R}^2 \mid \vartheta = \tanh(\varphi), \varphi \in [-20, 20]\}.$$

Since  $\tanh$  is an odd function, candidate generation is carried out on one half of the domain, and the remaining candidates are obtained by symmetry. In addition, we include the analytic

global constraint  $1 - \vartheta^2 \geq 0$ , which is valid on the graph of  $\tanh$  and therefore does not require SOS verification.

For the data-driven step, we use  $\rho = 10^{-3}$ ,  $\lambda_{\text{loc}} = 10$ ,  $\lambda_{\text{g}} = 1$ ,  $\lambda_{\text{ext}} = 10$ , and  $\bar{\gamma} = 10^{-2}$ , together with 5000 global samples. Candidate generation is performed on four subregions in the left half of the domain, namely  $[-4, -1.5]$ ,  $[-2, 0]$ ,  $[-2, -0.7]$ , and  $[-1.2, -0.5]$ . The first two subregions are used to generate upper bounding candidates, and the latter two are used to generate lower bounding candidates. The remaining candidates are then obtained by symmetry.

Since  $\tanh$  is nonpolynomial, the data-driven candidates are successfully verified using the procedure of Section III for nonpolynomial relations. For the SOS step, the interval  $[-20, 20]$  is partitioned into  $[-20, -5]$ ,  $[-5, -1]$ ,  $[-1, 1]$ ,  $[1, 5]$ ,  $[5, 20]$ . Constant functions are used on the first and fifth intervals, cubic polynomials are used on the second and fourth intervals, and a seventh-order Taylor approximation is used on  $[-1, 1]$ . The final family consists of the analytic global constraint and eight data-driven quadratic constraints.

- 2) *Unit saturation:* Consider the unit saturation function

$$\vartheta = \text{sat}(\varphi) := \begin{cases} -1, & \varphi \leq -1, \\ \varphi, & -1 \leq \varphi \leq 1, \\ 1, & \varphi \geq 1. \end{cases}$$

We consider its graph on the compact domain  $\varphi \in [-5, 5]$ . Since the function is odd, candidate generation is again carried out on one half of the domain, and the remaining candidates are obtained by symmetry.

The data-driven quadratic program is solved with  $\rho = 10^{-3}$ ,  $\lambda_{\text{loc}} = 10$ ,  $\lambda_{\text{g}} = 1$ ,  $\lambda_{\text{ext}} = 5$ , and  $\bar{\gamma} = 10^{-3}$ . We use 500 global samples and decompose the domain into three subregions,  $[-5, -1.2]$ ,  $[-1.5, -0.5]$ , and  $[-0.8, 0]$ , corresponding to the saturated branch, the corner region, and the linear region, respectively. For each subregion, the candidate is shaped using local samples together with uniformly generated exterior samples and selected target exterior points. The first two subregions are used to generate upper bounding candidates, while the third is used to generate a lower bounding candidate; the corresponding candidates on the other half of the domain are obtained by symmetry.

Unlike  $\tanh$ , the saturation function is piecewise affine and admits an exact semialgebraic description. Therefore, candidate generation and verification are carried out directly on the exact graph. The generated candidates are verified using the SOS feasibility problems. They are also verified in Frama-C [18] using the SMT solvers Z3 [19] and Alt-Ergo [20]. For the Rocq verification, using exact rational fractions and explicit algebraic identities eliminates the need for complex non-linear searches, allowing Rocq to verify the proof directly. The verification scripts and results are available in the GitHub repository.

To demonstrate the benefit of the proposed quadratic characterization for saturation, we consider the automobile active suspension example in [3] with the same parameter values, controller-synthesis, and uncertainty structure, consisting of an LTI uncertain parameter and a sector-bounded nonlinearity.

The latter is defined as a saturation nonlinearity acting on the control input. Minimum volume state-invariant ellipsoids are then computed using both the proposed characterization and the pointwise-IQC sector characterization of saturation with a locally tightened sector bound, following the methodology of [3]. In the pointwise-IQC approach, the sector characterization is enforced on the dead-zone representation associated with the saturation function, whereas our proposed characterization is imposed directly on the saturation input-output relation. The saturation limit is set to 100N in both cases. Fig. 2 shows the projections of the resulting invariant ellipsoids onto the  $(x_1, x_2)$ -plane. The ellipsoid obtained with the proposed characterization is less conservative and is contained in the pointwise-IQC ellipsoid. The corresponding  $-\log \det$  objective values for the augmented state ellipsoids are 30.95 and 41.73, respectively; for the Schur-complement projections, they are 9.71 and 14.6.

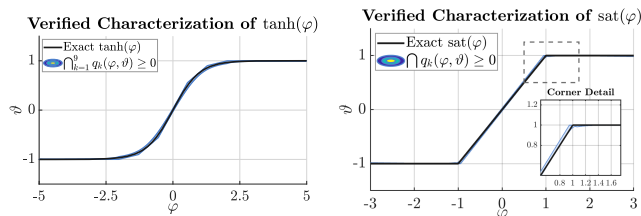


Fig. 1. Verified characterizations of  $\tanh(\cdot)$  (left) and  $\text{sat}(\cdot)$  (right).

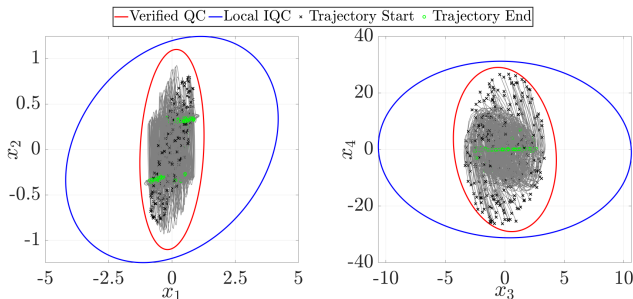


Fig. 2. Projections of the state-invariant ellipsoids and simulations in the  $(x_1, x_2)$  and  $(x_3, x_4)$  planes.

### B. Reachability analysis of a $\tanh$ neural-network controller

We consider the  $\tanh$  neural-network controller from [21], with 27 inputs, two hidden layers of 64 neurons each, and 4 outputs. The inputs are normalized measurements, so the admissible input set is

$$\mathcal{X} = \{x \in \mathbb{R}^{27} \mid \|x\|_\infty \leq 1\}.$$

The network outputs are control actions, which are post-processed before being applied to the system.

In this example, we use the verified  $\tanh$  characterization in Fig. 1 within the QC-based SDP formulation of Section IV. We compute output-reachability bounds and compare the resulting overapproximations against NNV [22], CORA [23], and  $\alpha, \beta$ -CROWN [24]. The plots in Fig. 3 show the reachable-set overapproximations in the  $(y_1, y_2)$  and  $(y_3, y_4)$  planes obtained using 180 polytope facets for all methods except CORA.

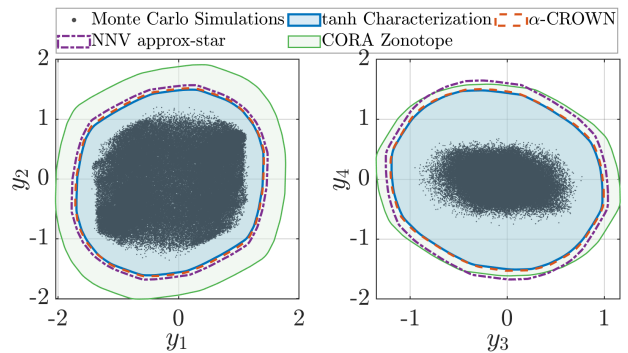


Fig. 3. Output reachable sets in the  $(y_1, y_2)$  and  $(y_3, y_4)$  planes.

On average, over all projection directions, the reachable-set widths obtained with the proposed characterization are approximately 6.4% tighter than those of NNV and approximately 1.2% tighter than those of  $\alpha, \beta$ -CROWN in this example. The bounds obtained with the proposed method were also independently verified using  $\alpha, \beta$ -CROWN. This illustrates that the adopted approach with the proposed characterization yields competitive results with current state-of-the-art tools.

### C. ReLU reachability and verification on ACAS Xu

We apply the ReLU-specific tightening methods of Section V to the ACAS Xu benchmark [25], [26], a standard neural-network verification benchmark for airborne collision avoidance. For simplicity, we refer to the joint use of the exact polynomial characterization of ReLU in (9) and the blockwise repeated-ReLU characterization defined by (10)–(11) as the combined characterization. For the reachability experiments, we consider the input set corresponding to Property  $\phi_1$  from [26] and compare the exact polynomial characterization with IBP local bounds (EP), the combined characterization with IBP local bounds (COMB), and the combined characterization with polytope propagation (COMB-PP) against NNV, CORA, and  $\alpha, \beta$ -CROWN. In the local bound tightening step, the normal vectors consist of the standard basis vectors, together with 25 right-singular vectors, and the repeated-ReLU maximum block size,  $s_{\max}$ , is set to 10. For simplicity, the quantitative comparison is reported for the first output only.

Table I reports the average output-interval width. The results show that COMB yields tighter bounds than EP, and that COMB-PP further improves these bounds. In particular, COMB-PP results in the smallest bounds on average among all methods considered. The effect of polytope propagation becomes more pronounced in deeper layers, where it mitigates the wrapping effect of IBP by tightening the local neuron bounds before the final output-reachability computation. In our experiments, the mean local-bound reduction relative to IBP is 41.3% at the fifth hidden layer and 67.3% at the sixth hidden layer. Stronger tightening can be obtained by using more normal vectors, such as ones encoding pairwise relations between neurons, or by increasing the repeated-ReLU block size, though both lead to higher computational cost. In particular, adding the aforementioned normal vectors, the deepest-layer mean local-bound reduction in our experiments reaches approximately 96–98% relative to IBP.

TABLE I

AVERAGE OUTPUT-1 INTERVAL WIDTHS FOR ACAS XU PROPERTY 1.

Method	Avg. width	Relative increase w.r.t. COMB-PP
<b>COMB-PP</b>	<b>93.06</b>	–
COMB	128.17	37.7%
EP	182.20	95.8%
NNV	331.96	256.7%
$\alpha, \beta$ -CROWN	373.26	301.1%
CORA	5241.52	5532.2%

Furthermore, using the proposed framework for property verification, we successfully verified Properties  $\phi_1$ ,  $\phi_3$ , and  $\phi_4$  of the ACAS Xu benchmark for all networks, with the property definitions taken from [26, Appendix VI]. Property  $\phi_1$  requires verifying that the first network output satisfies  $y_1 \leq 1500$  over the prescribed input set. Properties  $\phi_3$  and  $\phi_4$  require verifying that the first output  $y_1$  is not minimal for the corresponding input sets. This amounts to certifying the disjunctive condition  $\bigvee_{i=1}^4 (y_{i+1} \leq y_1)$ , or equivalently, that there exists at least one  $i \in \{1, \dots, 4\}$  such that  $y_{i+1} - y_1 \leq 0$ . In a branch-and-bound framework, this means that verification on a branch is complete once at least one of these inequalities is certified. This can be done in two ways: either by solving the feasibility problem associated with each condition separately, or by solving a single feasibility problem in which the term  $M_y$  in (5) is defined by

$$\xi^\top M_y \xi = \sum_{i=1}^4 \lambda_i (y_{i+1} - y_1),$$

where  $\lambda_i$  are nonnegative multipliers. If this latter problem is feasible with at least one nonzero multiplier, it follows that there exists at least one  $i \in \{1, \dots, 4\}$  such that  $y_{i+1} - y_1 \leq 0$ , which verifies the property on that branch.

## VII. CONCLUSION

This paper presents a framework for constructing verified quadratic characterizations of scalar static relations on bounded domains. The resulting verified quadratic constraints are directly compatible with existing QC- and pointwise-IQC-based analysis methods. When applied to neural-network reachability, the approach yields domain-dependent characterizations for smooth activations and reduces conservatism in feedforward ReLU networks. The examples demonstrate the effectiveness of the proposed methods on scalar nonlinearities, an uncertain-system example involving saturation, and neural-network reachability and verification benchmarks. Future work will explore applications to broader classes of uncertain nonlinear systems and the extension of the verification process to account for floating-point errors.

## REFERENCES

[1] A. Megretski and A. Rantzer, “System analysis via integral quadratic constraints,” *IEEE Transactions on Automatic Control*, vol. 42, no. 6, pp. 819–830, 1997.

[2] J. Veenman, C. W. Scherer, and H. Köroğlu, “Robust stability and performance analysis based on integral quadratic constraints,” *European Journal of Control*, vol. 31, pp. 1–32, 2016.

[3] E. Khalife, D. Abou Jaoude, M. Farhood, and P.-L. Garoche, “Computation of invariant sets for discrete-time uncertain systems,” *International Journal of Robust and Nonlinear Control*, vol. 33, no. 14, pp. 8452–8474, 2023.

[4] M. Fazlyab, M. Morari, and G. J. Pappas, “Safety verification and robustness analysis of neural networks via quadratic constraints and semidefinite programming,” *IEEE Transactions on Automatic Control*, vol. 67, no. 1, pp. 1–15, 2022.

[5] H. Hu, M. Fazlyab, M. Morari, and G. J. Pappas, “Reach-SDP: Reachability analysis of closed-loop systems with neural network controllers via semidefinite programming,” in *2020 59th IEEE Conference on Decision and Control (CDC)*, 2020, pp. 5929–5934.

[6] J. M. Fry, D. Abou Jaoude, and M. Farhood, “Robustness analysis of uncertain time-varying systems using integral quadratic constraints with time-varying multipliers,” *International Journal of Robust and Nonlinear Control*, vol. 31, no. 3, pp. 733–758, 2021.

[7] M. Putinar, “Positive polynomials on compact semi-algebraic sets,” *Indiana Univ. Mathematics Journal*, vol. 42, no. 3, pp. 969–984, 1993.

[8] P. A. Parrilo, “Exploiting algebraic structure in sum of squares programs,” in *Positive Polynomials in Control*, D. Henrion and A. Garulli, Eds. Springer Berlin Heidelberg, 2005, pp. 181–194.

[9] H. Yin, P. Seiler, and M. Arcak, “Stability analysis using quadratic constraints for systems with neural network controllers,” *IEEE Transactions on Automatic Control*, vol. 67, no. 4, pp. 1980–1987, 2022.

[10] S. V. Noori, B. Hu, G. Dullerud, and P. Seiler, “A complete set of quadratic constraints for repeated ReLU and generalizations,” *IEEE Transactions on Automatic Control*, pp. 1–14, 2025.

[11] C. Barrett and C. Tinelli, “Satisfiability modulo theories,” in *Handbook of Model Checking*. Springer Intl. Publishing, 2018, pp. 305–343.

[12] E. Khalife, P.-L. Garoche, and M. Farhood, “Code-level formal verification of ellipsoidal invariant sets for linear parameter-varying systems,” in *NASA Formal Methods*, K. Y. Rozier and S. Chaudhuri, Eds. Cham: Springer Nature Switzerland, 2023, pp. 157–173.

[13] —, “Formally proving invariant systemic properties of control programs using ghost code and integral quadratic constraints,” in *NASA Formal Methods*, A. Dutle, L. Humphrey, and L. Titolo, Eds. Cham: Springer Nature Switzerland, 2025, pp. 180–200.

[14] Y. Bertot and P. Castéran, *Interactive Theorem Proving and Program Development: Coq’Art: The Calculus of Inductive Constructions*, ser. Texts in Theoretical Computer Science. Springer Verlag, 2004.

[15] J. C. Mason and D. C. Handscomb, *Chebyshev Polynomials*. Chapman and Hall/CRC, 2002.

[16] S. Boyd, L. El Ghaoui, E. Feron, and V. Balakrishnan, *Linear Matrix Inequalities in System and Control Theory*. SIAM, 1994.

[17] J. Xue, J. Li, and Y. Gong, “Restructuring of deep neural network acoustic models with singular value decomposition,” in *Interspeech*, 2013, pp. 2365–2369.

[18] P. Cuoq, F. Kirchner, N. Kosmatov, V. Prevosto, J. Signoles, and B. Yakobowski, “Frama-C,” in *Software Engineering and Formal Methods*. Springer Berlin Heidelberg, 2012, pp. 233–247.

[19] L. de Moura and N. Björner, “Z3: An efficient smt solver,” in *TACAS’08/ETAPS’08*. Springer Berlin Heidelberg, 2008, pp. 337–340.

[20] S. Conchon, M. Iguernelala, and A. Mebsout, “A collaborative framework for non-linear integer arithmetic reasoning in Alt-Ergo,” in *2013 15th International Symposium on Symbolic and Numeric Algorithms for Scientific Computing*. IEEE, 2013, pp. 161–168.

[21] D. J. Marquis, B. Wilhelm, D. Muniraj, and M. Farhood, “Adversarial reinforcement learning for robust control of fixed-wing aircraft under model uncertainty,” in *Proceedings of the 2026 American Control Conference*, 2026, arXiv preprint arXiv:2510.16650.

[22] H.-D. Tran, X. Yang, D. Manzanos Lopez, P. Musau, L. V. Nguyen, W. Xiang, S. Bak, and T. T. Johnson, “NNV: The neural network verification tool for deep neural networks and learning-enabled cyber-physical systems,” in *Computer Aided Verification*, S. K. Lahiri and C. Wang, Eds. Springer International Publishing, 2020, pp. 3–17.

[23] M. Althoff, “An introduction to CORA 2015,” in *Proceedings of the 1st and 2nd Workshop on Applied Verification for Continuous and Hybrid Systems*. EasyChair, 2015, pp. 120–151.

[24] S. Wang, H. Zhang, K. Xu, X. Lin, S. Jana, C.-J. Hsieh, and J. Z. Kolter, “Beta-Crown: Efficient bound propagation with per-neuron split constraints for neural network robustness verification,” *Advances in Neural Information Processing Sys.*, vol. 34, pp. 29909–29921, 2021.

[25] K. D. Julian, J. Lopez, J. S. Brush, M. P. Owen, and M. J. Kochenderfer, “Policy compression for aircraft collision avoidance systems,” in *2016 IEEE/AIAA 35th Digital Avionics Systems Conference*, 2016, pp. 1–10.

[26] G. Katz, C. Barrett, D. L. Dill, K. Julian, and M. J. Kochenderfer, “Reluplex: An efficient smt solver for verifying deep neural networks,” in *Computer Aided Verification*, R. Majumdar and V. Kunčák, Eds. Springer International Publishing, 2017, pp. 97–117.